

1 **Impact of carbon nanotubes on bioaccumulation and translocation of**  
2 **phenanthrene, 3-CH<sub>3</sub>-phenanthrene and 9-NO<sub>2</sub>-phenanthrene in maize (*Zea***  
3 ***mays*) seedling**

4 Xilong Wang<sup>a,\*</sup>, Ye Liu<sup>a</sup>, Haiyun Zhang<sup>a</sup>, Xiaofang Shen<sup>a</sup>, Fei Cai<sup>a</sup>, Meng Zhang<sup>a</sup>,  
5 Qian Gao<sup>a</sup>, Weixiao Chen<sup>a</sup>, Bin Wang<sup>b</sup> and Shu Tao<sup>a</sup>

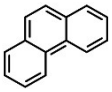
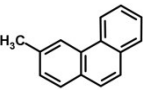

6 <sup>a</sup>Laboratory for Earth Surface Processes, College of Urban and Environmental  
7 Sciences, Peking University, Beijing 100871, China

8 <sup>b</sup>School of Public Health, Peking University, Beijing 100191, China

9  
10 \*Corresponding author: Phone: 86-10-62757822; Email: [xilong@pku.edu.cn](mailto:xilong@pku.edu.cn) (Xilong  
11 Wang)

12  
13  
14  
15  
16  
17 **Supporting Information**  
18

19 **Table S1.** Physicochemical properties of Phen, 3-CH<sub>3</sub>-Phen and 9-NO<sub>2</sub>-Phen

Chemicals	Chemical structure	MW	Log $K_{ow}$	$S_w$	Density	MV
Phen		178.23	4.46	1.15	1.063	169.5
3-CH <sub>3</sub> -Phen		192.26	5.15	0.28	1.100	185.3
9-NO <sub>2</sub> -Phen		223.23	1.96	1.67	1.300	191.7

MW: molecular weight (g/mol);  $K_{ow}$ : octanol-water partition coefficient;  $S_w$ : aqueous solubility (mg/L); density (g/cm<sup>3</sup>); and MV: molecular volume (Å<sup>3</sup>).

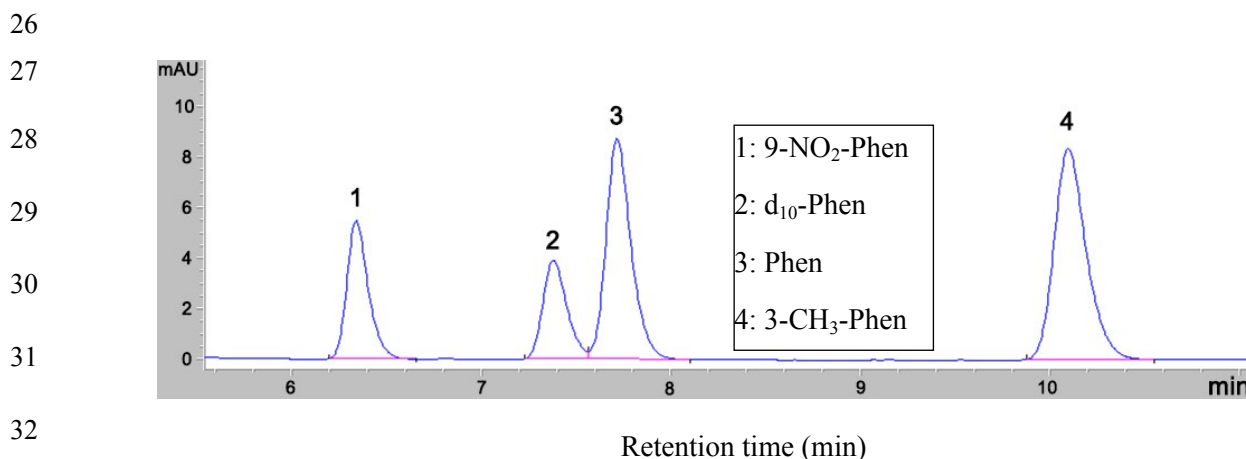
20  
21 **Table S2.** Elemental composition, surface area and porosity of the carbon nanotubes

Carbon nanotubes	Elemental composition (%)						Ash (%)	(O+N)/C	SA (m <sup>2</sup> /g)	Pore volume (cm <sup>3</sup> /g)	
	Bulk				Surface					$V_{mic}$	$V_{mes}+V_{mac}$
	C	H	N	O	C	O					
MW50	96.73	0.26	0.29	0.07	98.9	1.14	2.65	0.006	77	0.054	0.696
MW8	90.33	0.57	0.22	4.83	97.2	2.59	4.05	0.044	388	0.226	0.705
SW	93.47	0.38	0.22	2.01	97.8	2.22	3.92	0.020	495	0.215	1.48

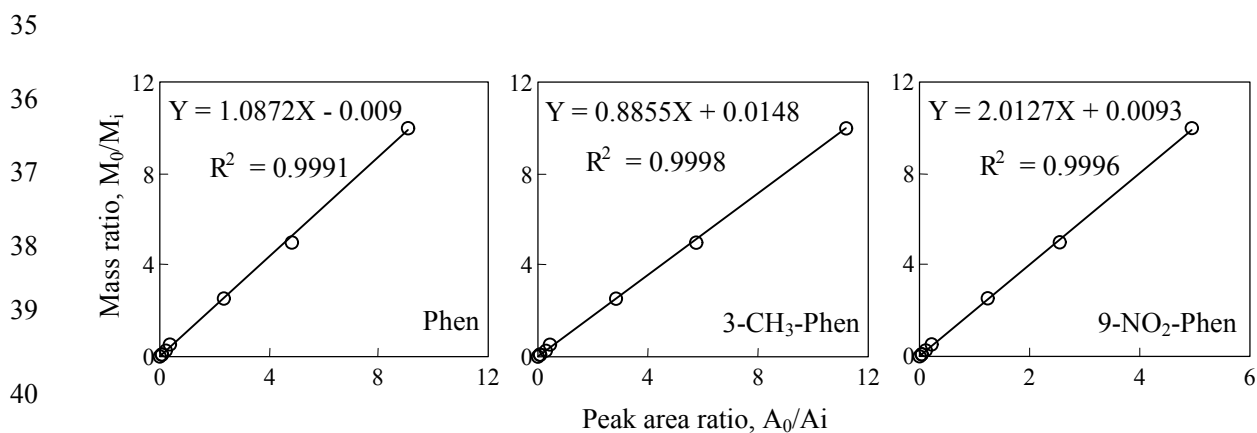
SA: surface area;  $V_{mic}$ : micropore volume; and  $V_{mes} + V_{mac}$ : a sum of meso- and macropore volumes.

24 **Table S3.** The characteristic HPLC/UV analytical parameters of Phen, 3-CH<sub>3</sub>-Phen, 9-NO<sub>2</sub>-  
 25 Phen

Chemicals	Retention time (min)	RSD, %	Detection limit (ng/g)	Recovery, % (n = 5)			
				Soil	RSD, %	Plant	RSD, %
Phen	7.710	0.57	4.23	73.5	4.06	78.0	3.48
3-CH <sub>3</sub> -Phen	10.094	0.50	1.25	89.1	6.58	92.3	5.16
9-NO <sub>2</sub> -Phen	6.339	0.73	9.23	101.7	7.88	100.7	3.69
d <sub>10</sub> -Phen	7.377	0.44	-	-	-	-	-



33 **Fig. S1** The peak profile of Phen, 3-CH<sub>3</sub>-Phen, 9-NO<sub>2</sub>-Phen, and the internal standard  
 34 d<sub>10</sub>-Phen in HPLC spectrum.



41 **Fig. S2** The standard curves for quantification of the tested compounds. Here, A<sub>0</sub> and  
 42 A<sub>i</sub> refer to the peak areas of the tested compound and internal standard, respectively.  
 43 The symbols M<sub>0</sub> and M<sub>i</sub> are masses of the tested compound (ng) and internal standard  
 44 (200 ng), respectively.

45  
 46  
 47

48  
49  
50  
51  
52  
53  
54  
55  
56  
57  
58  
59  
60  
61  
62  
63  
64  
65  
66  
67  
68  
69  
70  
71

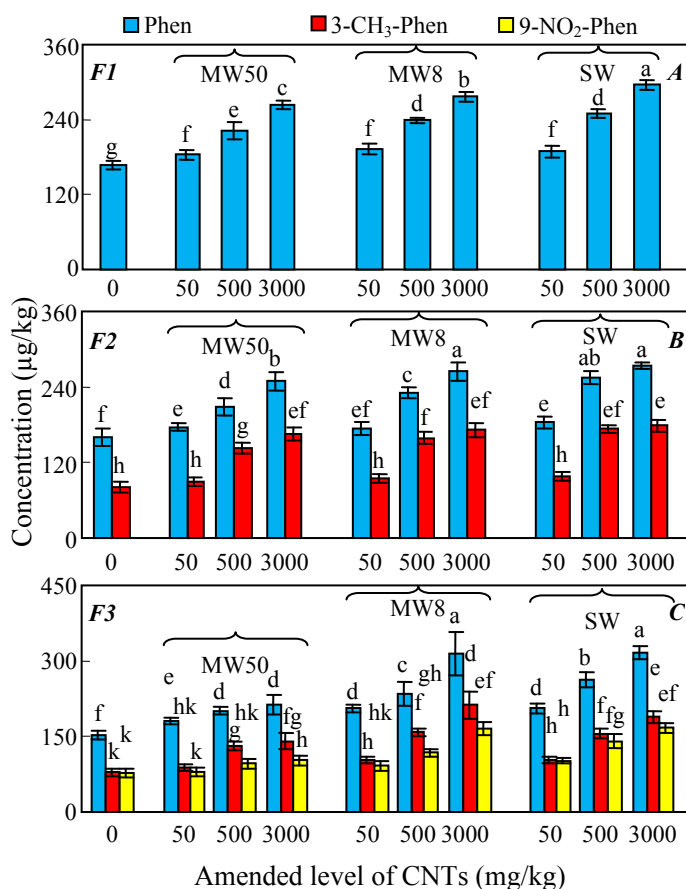


**Fig. S3** The residual concentration of Phen in soil in the F1 systems (A), Phen and 3-CH<sub>3</sub>-Phen in the F2 systems (B), as well as Phen, 3-CH<sub>3</sub>-Phen and 9-NO<sub>2</sub>-Phen in soil in the F3 systems (C). For a given panel, bars with different letters are significantly different ( $p < 0.05$ ). In contrast, if two bars are given the same letter or they have a common letter, they are insignificantly different at a significance level of 0.05.

72  
73  
74  
75  
76  
77  
78  
79  
80  
81  
82  
83  
84  
85

**Sorption Experiments.** All sorption isotherms of Phen, 3-CH<sub>3</sub>-Phen, and 9-NO<sub>2</sub>-Phen to the carbon nanotubes were obtained using a batch equilibration technique at room temperature ( $25 \pm 1$  °C). Due to low water solubility of 3-CH<sub>3</sub>-Phen in water, 100 mL screw cap vials were used, but 40 mL vials were used for Phen and 9-NO<sub>2</sub>-Phen; in consideration of high surface area of MW8 and SW, small mass of them were used to reach comparatively low solid-to-liquid ratio. For Phen and 9-NO<sub>2</sub>-Phen, 0.8 mg MW50, 0.3 mg MW8 and 0.3 mg SW with 40 mL background solution were added to each vial, respectively. For 3-CH<sub>3</sub>-Phen, 0.6 mg MW50, 0.3 mg MW8 and

0.3 mg SW with 100 mL background solution were mixed together, respectively. The composition of the background solution (pH = 7.0) contained 0.01 mol/L CaCl<sub>2</sub> to maintain a constant ionic strength and 200 mg/L NaN<sub>3</sub> to inhibit microbial activity. Initial concentrations of the tested compounds were established in 5 concentration gradients within the range of solubility. The volume fraction of methanol in test solution of each vial was controlled to be less than 0.1% to avoid cosolvent effect. The vials were sealed with aluminum foil before being covered with Teflon screw caps. These vials were then placed on a rotary shaker for 5 days. Our preliminary experiments showed that sorption equilibrium was reached within 4 days. After mixing, the vials were centrifuged at 3000 rpm for 20 min, the supernatant was taken and filtered with anodic alumina membrane (0.2 μm, Whatman International, Germany). The pH of the final test solution was measured and found to be unchanged in comparison with that of the initial one. The equilibrium concentrations of all compounds were determined with HPLC. According to the concentrations of control groups without containing carbon nanotubes, uncertainties of the concentrations of all tested compounds were less than 2% as compared to their initial ones. So the concentrations of the organic compounds were directly calculated by the HPLC measurement results.

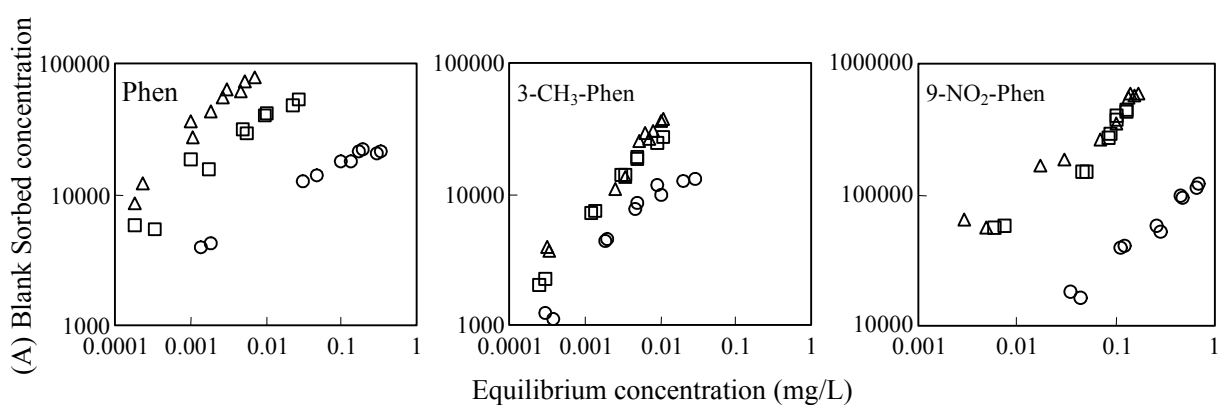


**Fig. S4** Sorption isotherms of Phen, 3-CH<sub>3</sub>-Phen and 9-NO<sub>2</sub>-Phen by various carbonaceous NPs. MW50 (○); MW8 (□); SW (△).

119  
120  
121  
122  
123  
124  
125  
126  
127  
128  
129  
130  
131  
132  
133  
134  
135  
136  
137  
138  
139  
140  
141  
142  
143  
144  
145  
146

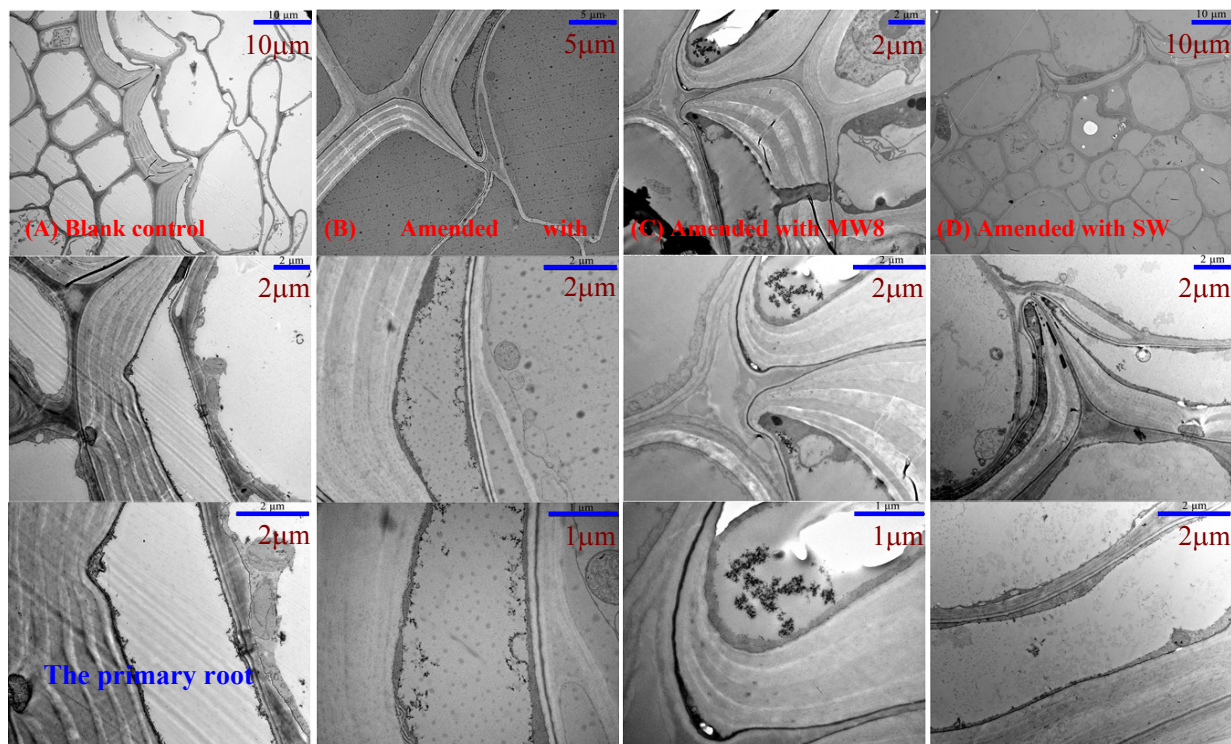


**Fig. S5** The TEM images of the casparian strip of the primary roots of maize seedling of the blank control and those from the systems amended with CNTs at various scales.



148

149

150

151

152

153

154

155

156

157

158

159

160

161

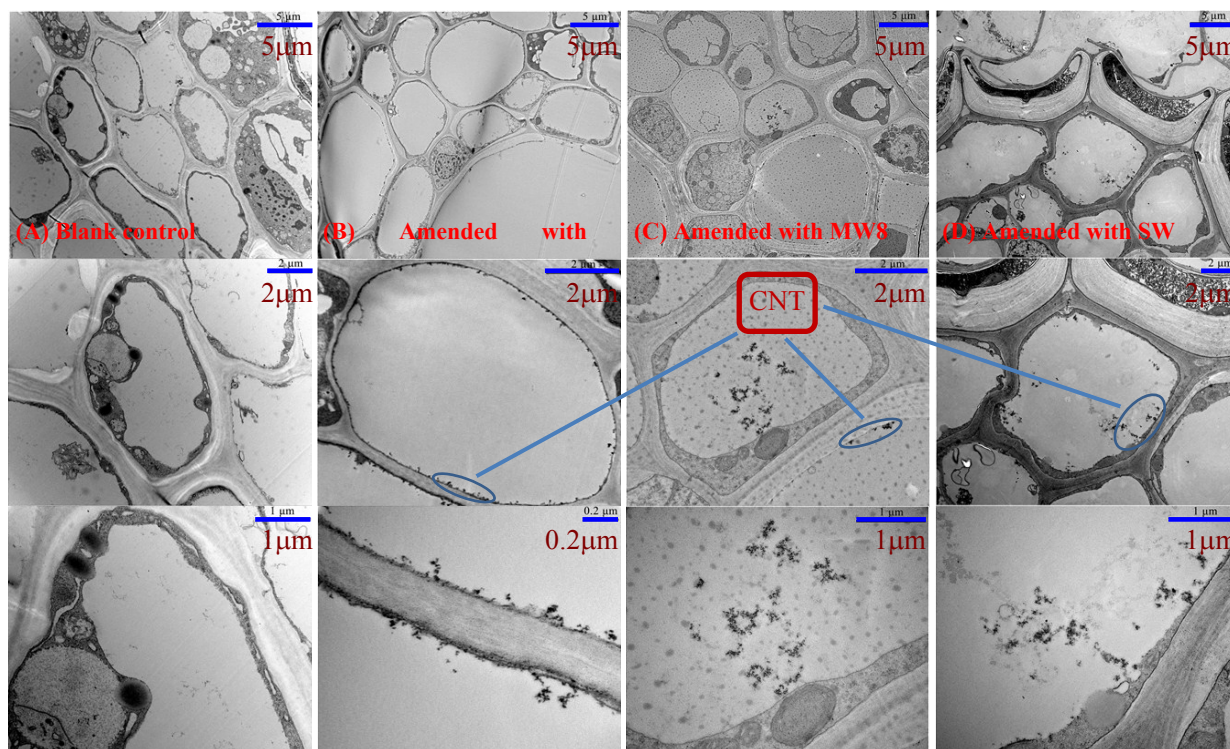
162

163

164

165

166



167

168 **Fig. S6** The TEM images of the phloem of the secondary roots of maize seedling of control and  
169 those from the systems amended with CNTs at various scales.

170

171

172

173

174

175

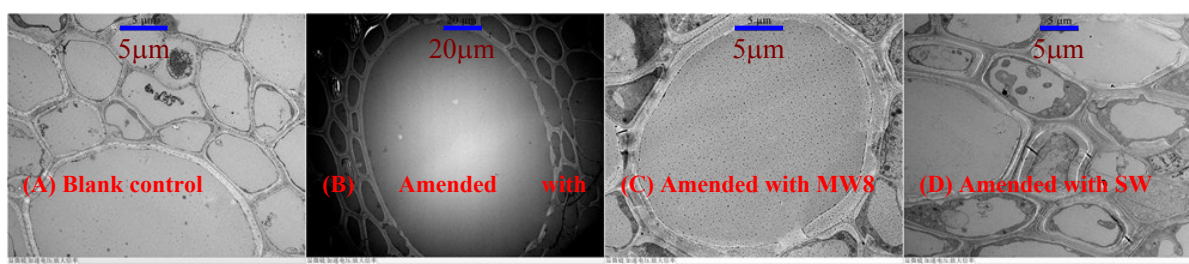
176

177

178

179

180



181 **Fig. S7** The TEM images of the xylem of the secondary roots of maize seedling of the blank  
182 control and those from the systems amended with CNTs.

183



185

186

187

188

189

190

191

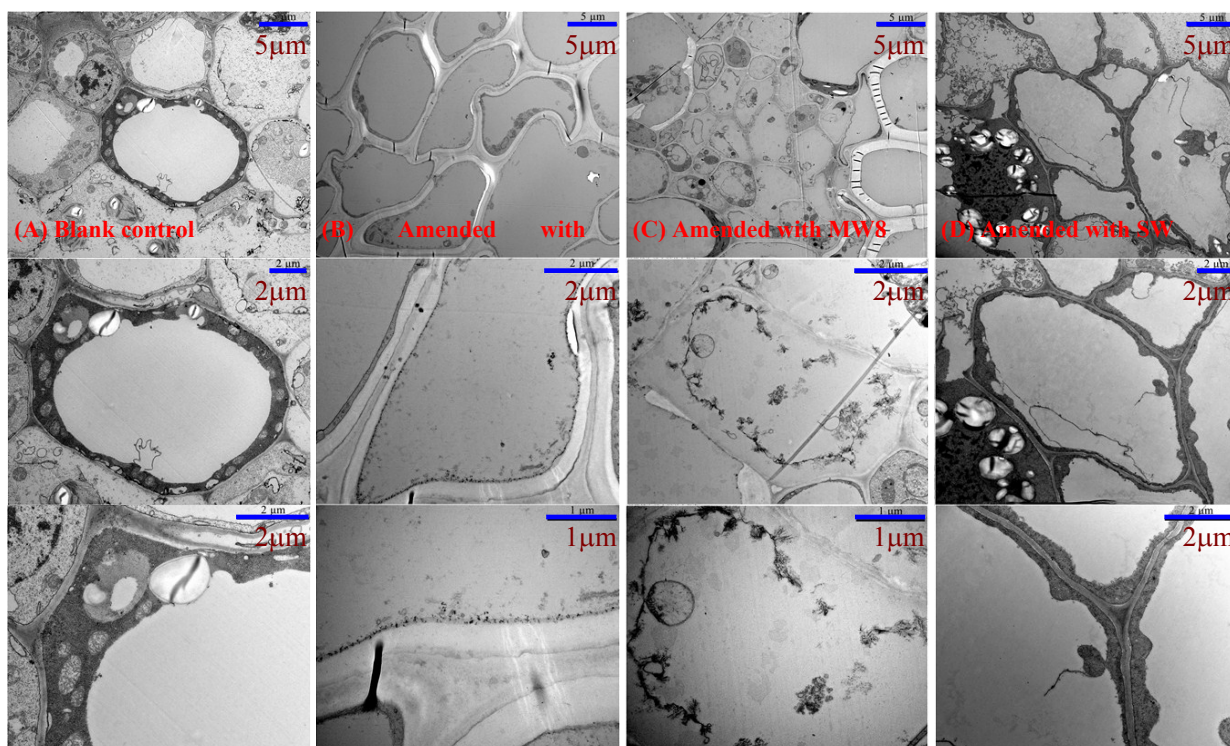
192

193

194

195

196



197 **Fig. S8** The TEM image of the maize seedling stem from control and the systems  
198 amended with CNTs at various scales.

199

200

201

202

203

204

205

206

207

208

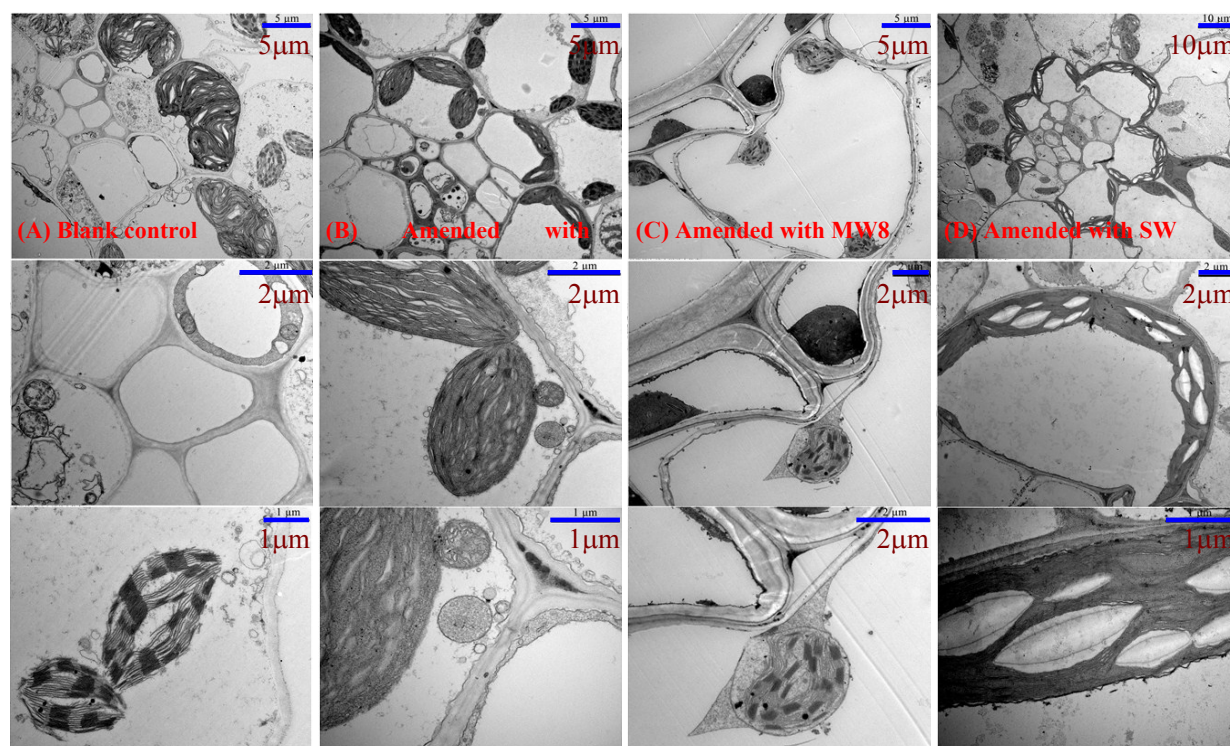
209

210

211

212

213



214 **Fig. S9** The TEM images of the maize seedling leaves from control and the systems amended  
215 with CNTs at various scales.